

Jet Production in the More Extended Extragalactic Radio Sources and Unification with Compact Steep Spectrum Sources

Jeremiah Chukwuemerie Ezeugo, Ph.D.

Department of Physics and Industrial Physics, Nnamdi Azikiwe University, Awka, Anambra State, Nigeria.

E-mail: chuksemerie@yahoo.com

ABSTRACT

Analytical methods and simple linear regression analyses have been used in this paper to show the possibility that jet production by magnetization predominates over other mechanisms of jet production in the more extended extragalactic radio sources (EGRS) with low power output. We estimate accretion-induced magnetic field and jet-driving magnetic field of some more extended EGRS in our sample. A possible implication of the results obtained through simple linear regression analyses of data estimated for the two aforementioned fields, is that jet production by magnetization predominates in the more extended EGRSs with lower power output; while in those sources with higher power output, the converse may be the case. That is, other processes, such as, hydrodynamic, thermal, and radiation pressures may predominate over jet magnetization. Similar results were obtained by [10] for the compact steep spectrum sources (CSS). This similarity between these two sources – the more extended EGRS and CSS – simply suggests that CSS sources are simply scaled-down versions of the more extended EGRS.

(Keywords: jet, magnetization, radio sources, accretion, magnetic field)

INTRODUCTION

Extragalactic radio sources (EGRS) are those sources with a high ratio of radio to optical emission, commonly defined by the ratio of the two flux densities, $S_{5\text{ GHz}}/S_{6 \times 10^5\text{ GHz}} > 10$ [1]. They are located beyond the confines of our galaxy – the Milky Way. They consist of radio galaxies, radio quasars and BL Lacertae objects [2–3]. Radio emission from these sources usually takes the form of two opposite sided relativistic jets that connect the base of the accretion disk to two radio-emitting lobes that straddle the central

component that is more or less coincident with the nucleus of the host galaxy [2, 4-6]. In some sources, the lobes contain hotspots believed to be the termination points of the jets [2, 4–6] (Figures 1 and 2).

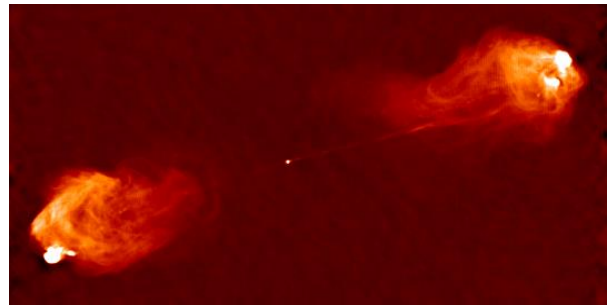


Figure 1: Cygnus A – An EGRS.
Source: Wikipedia

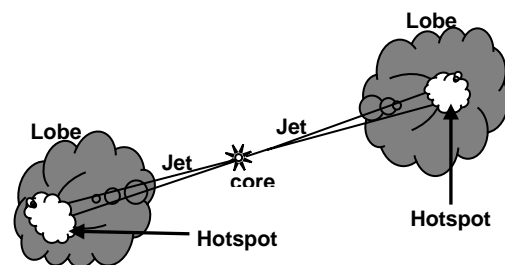


Figure 2: The Structure of a Typical EGRS.
Source: the author.

The more extended EGRS have linear sizes, D , given by $D > 20\text{ Kpc}$ assuming Hubble constant, $H_0 = 75\text{ kms}^{-1}\text{Mpc}^{-1}$. In most cases, their linear sizes extend into intergalactic media. Their radio luminosity is in excess of 10^{26} W at 5 GHz and overall luminosities ($P_{bol} \geq 10^{37}\text{ W}$) in common with the Compact Steep Spectrum Sources (CSS) [3, 7].

On the other, CSS sources are full-fledged EGRS. Their properties are as follows [7–8]: (i) they are assumed to be normal EGRS but miniaturized – their observed linear sizes, $D \leq 20$ kpc; (ii) they consist of both radio galaxies and radio-loud quasars but on sub-galactic dimensions; (iii) they show steep spectra ($\alpha \geq 0.5, S_\nu \sim \nu_p^\alpha$) at high frequencies (e.g. ≥ 0.02 GHz) from the entire radio morphological structures; (iv) they have high radio luminosities, $P_{5\text{ GHz}} \geq 10^{21}$ W; and overall luminosities, $P_{\text{bol}} \geq 10^{37}$ W.

Many authors have wondered on the connection between CSS sources and the more extended EGRS. As a result, there are models for the evolution of CSS sources in the literature. These include: Youth Scenario (i.e., young evolving sources), Frustration Scenario (i.e., sources confined by ambient dense gases), Relativistic Beaming and Orientation Effects (i.e., the source sizes are foreshortened by orientation and projection effects) [7–9].

In this work, we use analytical methods to estimate accretion-induced magnetic field and jet-driving magnetic field of some more extended EGRS in our sample. We use the estimates to find if there is any relation between magnetic field possibly responsible for jet formation and that induced by accretion process. We compare the results with those obtained by [10].

We have not applied full magneto-hydrodynamic equations which may be considered appropriate in describing the phenomena of accretion and jet production [11–14]. However, for the purpose of obtaining a simple relation between the two fields, we have applied electrostatics in our derivations.

The radio sources used in the analyses were obtained from [15]. They are made up of 31 EGRS (radio galaxies) with linear sizes, $D > 30$ kpc. These sources are those whose jets have estimated velocities from [16].

ACCRETION-INDUCED AND JET-DRIVING MAGNETIC FIELDS

The most accepted model in the description of astrophysical jet formation is the magnetic acceleration model [11–14]. This states that bipolar relativistic jets are powered by magnetic fields tightly twisted by differential rotation of accretion disk [11]. Moreover, it has been pointed out that the terminal velocity of a jet

is in consonance with the rotational velocity of the disk at the foot of the jet [11]. This simply suggests that relativistic jet is produced at a position very close to the event horizon of the black hole residing at the central core of the EGRS.

It is commonly believed that accretion disk consists of plasma (i.e., positive ions and electrons). This implies that the effective axial magnetic field generated may either cancel out (assuming equal number of accreting opposite charges) or highly reduced when compared to the field produced if the disc were made up of an ensemble of like charges. However, for the purpose of finding the behavior of jet-driving magnetic field in relation to accretion-induced magnetic field, we assume the disk comprises an ensemble of equal positive and negative charges.

Here, we are interested in the resultant magnetic field induced by the motion of plasma in the accretion disk at the disk center (assumed here to cover the entire diameter of the event horizon).

Therefore, approximating the ensemble of negative charges present in the disk to a current-carrying thick hollow circular disc as shown in Figures 3 and 4, then by Biot-Savart law, it can be shown that magnetic field, B_{acc} , produced at the center of the disk by electrons in the accreting plasma can be expressed as:

$$B_{\text{acc}} \approx \int_{R_a}^{R_b} \int_0^x \left(\frac{\mu_0 I}{2R} \right) dR dx \quad (1)$$

where, $\frac{\mu_0 I}{2R}$ = magnetic field at the center of a
current-carrying narrow circular ring
 R_a = inner radius
 R_b = outer radius
 I = total electric current due to the
motion of the negative charges (or
electrons) in the accreting plasma
 R = radius of the disc
 x = thickness of the disk

On integration, (1) yields:

$$B_{\text{acc}} \approx \frac{\mu_0 I x}{2} \ln(R_b - R_a) \quad (2)$$

Applying the general definition of electric current and considering accretion over the source dynamical age, T , (2) may be rewritten as:

$$B_{acc} \approx \frac{\mu_0 N e x}{2T} \ln(R_b - R_a) \quad (3)$$

where, N = number of electrons in the disc
 e = electronic charge.

An accretion disk has inner radius whose value may lie between $\approx 1R_s$ and $\approx 10R_s$ depending on the type of disk [3]. R_s is Schwarzschild radius or event horizon. The outer radius of accretion disk may extend to $10^4 R_s$ [3].



Figure 3: An Accretion Disk.
 Source: Wikipedia.

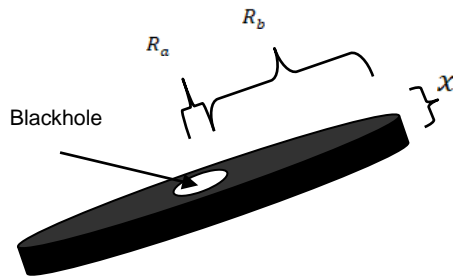


Figure 4: Schematic Diagram of an Accretion Disk. Source: the author.

Taking the mean, R_a becomes $5R_s$; while R_b gives $10^4 R_s$. Putting the values in (3) yields:

$$B_{acc} \approx \frac{\mu_0 N e x}{2T} \ln(9,995 R_s) \quad (4)$$

Combining the expression relating Schwarzschild radius to black hole mass, M_b ; that is [3, 17],

$$R_s = \frac{2GM_b}{c^2} \quad (5)$$

where, G = universal gravitational constant
 c = light speed

with (4) and (5), we obtain:

$$B_{acc} \approx \frac{\mu_0 N e x}{2T} \ln\left(19,9950 \left[\frac{GM_b}{c^2}\right]\right) \quad (6)$$

For simplicity, assuming a source radiating at Eddington limit, the power, L_{Edd} , radiated is given by [3]:

$$L_{Edd} = \frac{4\pi GM_b m_H c}{\sigma_T} \quad (7)$$

L_{Edd} is in watts, M_b is in kg, m_H (proton mass) is in kg and σ_T is Thompson interaction cross-section. Approximating Eddington luminosity to source bolometric luminosity, P_{bol} , the last equation becomes:

$$M_b \approx \frac{P_{bol} \sigma_T}{4\pi G m_H c} \quad (8)$$

Putting it in (6), gives:

$$B_{acc} \approx \frac{\mu_0 N e x}{2T} \ln\left(4,997.5 \left[\frac{P_{bol} \sigma_T}{\pi m_H c^3}\right]\right) \quad (9)$$

Moreover, number of electrons, N , in an accretion disk in relation to the particle number density, n_{acc} , of the accreting electrons can be written by:

$$N = n_{acc} \pi x (R_b^2 - R_a^2) \quad (10)$$

which yields:

$$N \approx 10^8 \pi x R_s n_{acc} \quad (11)$$

Combining (5) and (11), we obtain:

$$N \approx 10^8 \pi x n_{acc} \left(\frac{2GM_b}{c^2}\right) \quad (12)$$

Also, combining (8) and (12) gives:

$$N \approx (5 \times 10^7) \frac{x n_{acc} P_{bol} \sigma_T}{c^3 m_H} \quad (13)$$

Substituting for N in (9) yields:

$$B_{acc} \approx 2.5 \times 10^7 \frac{\mu_0 e x^2 n_{acc} P_{bol} \sigma_T}{c^3 m_H T} \ln \left(4,997.5 \left[\frac{P_{bol} \sigma_T}{\pi m_H c^3} \right] \right) \quad (14)$$

This implies that magnetic field induced at the center of an accretion disk (for negative charges only) of an extragalactic radio source may be estimated if the thickness (x) of the disk and electron number density (n_{acc}) are known.

For simplicity, we assume a thin disc with [14]:

$$\frac{\left(\frac{x}{2}\right)}{R_a} \approx 0.05 \quad (15)$$

where R_a = distance between the central core and the thin disk (Figure 4).

Combining the last equation (having assumed for simplicity that $R_a \approx R_s$) with (5) and (8), x becomes:

$$x \approx 0.05 \left(\frac{P_{bol} \sigma_T}{\pi m_H c^3} \right) \quad (16)$$

Substituting for x in (14), we obtain:

$$B_{acc} \approx 6.25 \times 10^4 \frac{\mu_0 e \sigma_T^3 n_{acc} P_{bol}^3}{\pi^2 c^9 m_H^3 T} \ln \left(4,997.5 \left[\frac{P_{bol} \sigma_T}{\pi m_H c^3} \right] \right) \quad (17)$$

Moreover, jet-driving magnetic field, B_{jet} , can be expressed as [18]:

$$B_{jet} \approx \frac{m_H c n_e \Omega V_j T}{(1.6 \times 10^{-5}) \pi n_{jet} e D^2} \quad (18)$$

where, n_e = source ambient density

Ω = jet opening solid angle

V_j = jet velocity

n_{jet} = jet internal density

D = source observed linear size

Assuming jet density approximate to ambient medium density, (18) becomes:

$$B_{jet} \approx \frac{m_H c \Omega V_j T}{(1.6 \times 10^{-5}) \pi e D^2} \quad (19)$$

ANALYSES AND RESULTS

In this section, we want to estimate the two quantities, B_{acc} and B_{jet} in (17) and (19) respectively; after which we find if there is any relationship between them using a simple regression analyses. Taking typical values of the following quantities:

$$\begin{aligned} m_H &= 1.67 \times 10^{-27} \text{kg} \\ e &= 1.602 \times 10^{-19} \text{C} \\ c &= 3 \times 10^8 \text{m/s} \\ \Omega &= 3.6 \times 10^{-5} \text{sr} \\ V_j &\approx 0.3c \text{ [23]} \\ m_e &= 9.109 \times 10^{-31} \text{kg} \\ \mu_0 &= 4\pi \times 10^{-7} \text{Hm}^{-1} \\ \sigma_T &= 2.5 \times 10^{-29} \text{m}^2 \\ n_{acc} &\approx 10^{16.12} \text{ particles/cm}^3 \text{ [19].} \end{aligned}$$

we obtain the following equations:

$$B_{acc} \approx (6.925 \times 10^{-87.88}) \frac{P_{bol}^3}{T} \ln(8.82 \times 10^{-25} P_{bol}) \quad (20)$$

and

$$B_{jet} \approx (2.0158 \times 10^8) \frac{T}{D^2} \quad (21)$$

Using the values of source observed linear size (D), bolometric luminosity (P_{bol} [= Pv , where P and v are respectively observed source luminosities and observing frequency]), source ages (T) estimated by simply getting the quotients of the observed source linear sizes and their corresponding jet velocities obtained from [16], we estimate the two quantities, B_{acc} and B_{jet} .

We show $B_{acc} - B_{jet}$ plot in Figure 5. The result of the linear regression gives:

$$\text{Log} B_{jet} = 22.25 - 0.07 \text{Log} B_{jet} \quad (23)$$

with correlation coefficient, $r \approx 0.44$ which is marginal. Also, we carried out a simple linear regression analysis of $P - B_{jet}$ plot as shown in Figure 6. Result gives:

$$\text{Log} P_{bol} = 67.07 - 0.71 \text{Log} B_{jet} \quad (24)$$

with $r \approx 0.41$ which is also marginal. The results are discussed in the next section.

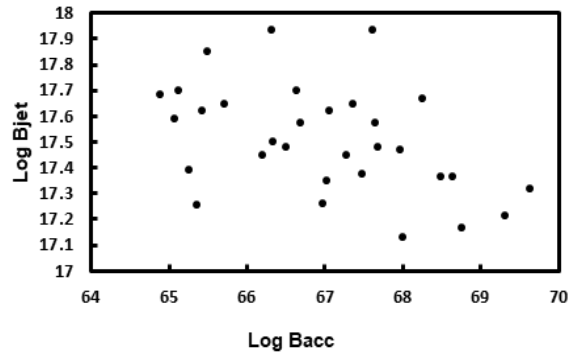


Figure 5: The Scatter Plot of Jet-Driving Magnetic Field against Accretion-Induced Magnetic Field.

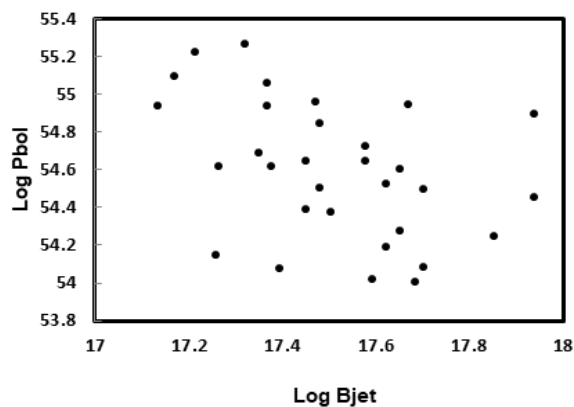


Figure 6: The Scatter Plot of Source Bolometric Luminosity against Jet-Driving Magnetic Field.

while in those sources with higher power output, the converse may be the case – some processes, such as; hydrodynamics, thermal, and radiation pressures may predominate over magnetization.

Moreover, Figure 7 is the plot of B_{acc} and B_{jet} against observed bolometric luminosities of the radio sources on the same axes. It compares B_{acc} and B_{jet} as P_{bol} increases. It shows that as luminosity grows, accretion-induced magnetic field at the center of accretion disk increases too, while jet-driving magnetic field decreases.

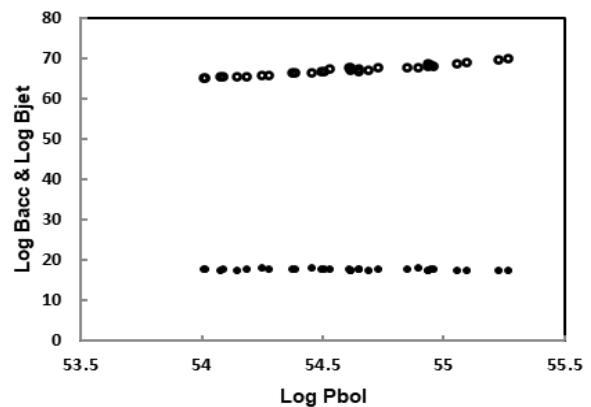


Figure 7: Scatter Plot of Accretion-Induced Magnetic Field (open circles) against Jet-Driving Magnetic Field (filled circles).

DISCUSSION AND CONCLUSION

We have estimated accretion-induced and jet-driving magnetic fields in the previous section. We use the estimates to find through linear regression analyses of $B_{acc} - B_{jet}$ data (Figure 5), a relation given by $B_{jet} \sim B_{acc}^{0.07}$, with correlation coefficient, $r \approx 0.44$. If we assume this marginal correlation is enough for observed sources, then we may state that the relation suggestively implies that jet production is predominated by magnetization in the sources with lower power output. Moreover, we find through similar regression analyses of $P_{bol} - B_{jet}$ data (Figure 6), a relation of the form, $P_{bol} \sim B_{jet}^{-0.712}$ (with $r \approx 0.41$) between the source observed bolometric luminosities and their corresponding estimated jet-driving magnetic fields.

A possible implication of these results is that jet production by magnetization predominates in the more extended EGRS with lower power output;

The results obtained are comparable with those obtained by [10] for the CSS sources. This similarity between these two sources – the large EGRS and CSS – simply suggests that CSS sources are simply miniaturized versions of the more extended EGRS.

REFERENCES

1. Urry, C.M. 2004. "AGN Unification: An Update". *Astronomical Society of the Pacific conference series 1*.
2. Readhead, A.C. 1995. "Evolution of Powerful Extragalactic Radio Sources". *In proc. Colloquium on Quasars and Active Galactic Nuclei, ed. Kohen, M., and Kellermann, K. National Academy of Sciences: Berkman Center, Irvine, CA. 92: 11447–11450*.

3. Robson, I. 1996. *Active Galactic Nuclei*. John Wiley and Sons Ltd.: London, UK.
4. Jackson, J.C. 1999. "Radio Source Evolution and Unified Schemes". *Publications of Astronomical Society of the Pacific*. 16: 124–129.
5. Kawakatu, N. and M. Kino. 2007. "The Velocity of Large-scale Jets in a Declining Density Medium". *In Serie de Conferencias. Triggering Relativistic Jets, ed. W.H. Lee and E. Ramirez-Ruiz*. 27: 192–197.
6. Ezeugo, J.C. and A.A. Ubachukwu. 2010. "The Spectral Turnover–Linear Size Relation and the Dynamical Evolution of Compact Steep Spectrum Sources". *Monthly Notices of the Royal Astronomical Society*. 408: 2256–2260.
7. O'Dea, C.P. 1998. "The Compact Steep Spectrum and Gigahertz Peaked Spectrum Radio Sources". *Publications of the Astronomical Society of the Pacific*. 110: 493–532.
8. Fanti, C., R. Fanti, D. Dallacasa, R.T. Schillizzi, R.E. Spencer, and C. Stanghellini, 1995. "Are Compact Steep Spectrum Sources Young"? *Astronomy and Astrophysics*. 302: 317–326.
9. Fanti, C., F. Pozzi, D. Dallacasa, R. Fanti, L. Gregorini, C. Stanghellini, and M. Vigotti. 2001. "Multi-frequency VLA Observations of a New Sample of CSS/GPS Radio Sources". *Astronomy and Astrophysics*. 369: 380–420.
10. Ezeugo, J.C. 2015. "On Compact Steep Spectrum Sources and Jet Production". *American Journal of Astronomy and Astrophysics*. 3: 1–5.
11. Koide, S., S. Shibata, and T. Kudoh. 1999. "Relativistic Jet Formation from Blackhole Magnetized Disk". *The Astrophysics Journal*. 522: 727–752.
12. Blandford, R.D. and D.G. Payne. 1982. "Hydrodynamic Flows from Accretion Disks and the Production of Radio Jets". *Monthly Notices of the Royal Astronomical Society*. 199: 883–903.
13. Ustyugova, G.V., A.V. Koldoba, M.M. Romanova, V.M. Chechetkin and R.V.E. Lovelace. 1995. "Magnetohydrodynamic Simulations of Outflows from Accretion Disks". *Astrophysics Journal*. 439: L39–L42.
14. Pringle, J.E. 1981. "Accretion Disk in Astrophysics". *Annual Reviews of Astronomy and Astrophysics*. 19: 137–162.
15. Nilsson, K. 1998. "Kinematical Models of Double Radio Sources and Unified Scheme" *Monthly Notices of the Royal Astronomical Society*. 132: 31–37.
16. O'Dea, C.P., R.A. Daly, P. Kharb, K.A. Freeman and S.A. Baum, S.A. 2009. "Physical Properties of Very Powerful FR II Radio Galaxies". *Astronomy and Astrophysics*. 336: 69–79.
17. Paczynsky, B. and P.J. Wiita. 1980. "Thick Accretion Disks and Supercritical Luminosity". *Astronomy and Astrophysics*. 88: 23 – 31.
18. Ezeugo, J.C. 2015. "Compact Steep Spectrum Sources and Ambient Medium Density". *International Journal of Astrophysics and Space Science*. 3: 1–6.
19. Weber, P. 2017. *The Density in the Accretion Disk of the Active Galactic Nucleus*. Friedrich-Alexander-University Erlangen. Nurnberg, Germany.

ABOUT THE AUTHOR

Dr. Jeremiah Chukwuemerie Ezeugo, is a Lecturer in the Department of Physics and Industrial Physics, Nnamdi Azikiwe University, Awka, Anambra State, Nigeria. He holds a Ph.D. degree in Astrophysics from the University of Nigeria, Nsukka. His research interests are in the areas of extragalactic radio astronomy and cosmology.

SUGGESTED CITATION

Ezeugo, J.C. 2021. "Jet Production in the More Extended Extragalactic Radio Sources and Unification with Compact Steep Spectrum Sources". *Pacific Journal of Science and Technology*. 22(1):14-19.

